



Improving outdoor human-thermal environment by optimizing the reflectance of water-retaining pavement through subjective field-based measurements

Yasuhiro Shimazaki^{a,b,*}, Masashige Aoki^c, Kenji Karaki^c, Atsumasa Yoshida^d

^a Department of Architecture and Civil Engineering, Toyohashi University of Technology, 1-1 Hibarigaoka, Tempaku-cho, Toyohashi, Aichi, 441-8580, Japan

^b Department of Human Information Engineering, Okayama Prefectural University, 111 Kuboki, Soja, Okayama, 719-1197, Japan

^c Taisei Rotec Corporation, 1456 Kamiya, Konosu, Saitama, 365-0027, Japan

^d Department of Mechanical Engineering, Osaka Prefecture University, 1-1 Gakuen-cho, Sakai, Osaka, 599-8531, Japan

ARTICLE INFO

Keywords:

Human-energy balance
Field experiment
Pedestrian surfaces
Thermal comfort
Cool material
Evaporation

ABSTRACT

The role of urban surfaces in climate is recognized worldwide. Cool pavements such as reflective and water-retaining pavements contribute to the mitigation of urban heat. To optimize the cooling performance of a combination of reflective and evaporative characteristics, water-retaining (WR) pavements, with reflectance values of 13% (WR13) and 25% (WR25), were used and compared to a conventional asphalt pavement (AS). In addition to measuring surface and atmospheric temperatures, human-energy balance known as “human-thermal load” was assessed using perceptive responses obtained from participants ($n = 78$). Experimental insolation conditions were classified as low-, medium-, and high-based on radiation effects. Water-retaining pavements demonstrated significant surface temperature reductions compared to the overall AS; however, air temperature and humidity above the pavement were less sensitive, and they were not significantly different between the two distinct pavements. Under high insolation, local thermal comfort improved and skin temperatures of the lower body reduced. These consequently reduced the temperature perceived in the whole-body and improved the thermal environment on the surface of WR13. These results can be reasonably explained using the human-thermal load. The increase in thermal load from reflected solar radiation is limited below a certain level of insolation. The overall radiation received by WR13 was moderate from both ground-reflected and -sourced infrared radiation sources. The human-thermal load of WR13 was significantly different from that of AS under high insolation. A modest reflective pavement, such as WR13, is anticipated to improve human thermal comfort.

1. Introduction

Urban heat islands (UHIs) and global warming affect life. Extreme increases in temperature pose health risks caused by heat exposure. In fact, heat waves have increased in frequency since the mid-20th century [1], and heat-related illness and even mortality during hot weather occur worldwide [2]. Urban climate change has affected the urban thermal environment more directly than global climate change; therefore, the thermal environment requires serious attention [3].

Anthropogenic activities in urban areas are major contributors to environmental issues such as UHIs [4]. Thermal conditions in urban areas are physically influenced by urban structures such as settlement

geometry, open spaces, and surface materials [5]. The influence of urban surfaces on urban climate is widely recognized; for instance, paved asphalt roads and concrete buildings absorb and retain solar heat within specific urban geometries, and consequently, they warm near-surface air. Mitigation of the UHI effect can be achieved using cool materials [6,7]. Cool pavements can significantly contribute to the mitigation of urban heat as pavements account for a high percentage of urban surfaces. Cool pavement technologies can create cooler surfaces by raising solar reflectance (albedo) or enabling evaporative cooling (water retention (WR) or permeability) [8]. As surface temperatures and near-surface air temperatures depend on incoming solar radiation, most existing research on cool pavements focus on solar reflectance as the

Abbreviations: AS, asphalt pavement; UHI, urban heat island; UTCI, universal thermal climate index; WBGT, wet-bulb globe temperature; WR, water-retaining.

* Corresponding author. Department of Architecture and Civil Engineering, Toyohashi University of Technology, 1-1 Hibarigaoka, Tempaku-cho, Toyohashi, Aichi, 441-8580, Japan.

E-mail address: shimazaki@ace.tut.ac.jp (Y. Shimazaki).

<https://doi.org/10.1016/j.buildenv.2021.108695>

Received 7 October 2021; Received in revised form 16 December 2021; Accepted 17 December 2021

Available online 21 December 2021

0360-1323/© 2021 Elsevier Ltd. All rights reserved.

primary determinant. Reflective cool pavements can be easily applied to both new and existing pavements [8]. The evaporation process requires a large amount of heat; therefore, evaporation of water on a pavement surface or within the void structure of the pavement can draw out heat from the pavement, which can reduce near-surface air temperatures [9].

Several studies on cool pavements have been reported for urban microclimates. Normally, they measure or predict physical environmental parameters such as surface, air temperature, and mean radiant temperature [10,11]. They may also conduct thermal assessments using thermo-physical indices, particularly the universal thermal climate index (UTCI), which is derived from physical environmental quantities [12]. In terms of pavement evaluation, lowering urban temperatures is important; this can directly help improve thermal conditions and reduce energy demands for air-conditioning [6,13]. As pavements are spaces occupied by humans, an appropriate human-thermal environment is essential. Only some studies have addressed field measurements with their occupants. Moreover, because of the variation in the threshold of in different regions [14], data from the occupants' subjective responses were used to explore thermal adaptation strategies.

Since the combined effects of reflective and evaporative pavements are hardly examined, Shimazaki et al. [15] conducted field investigations wherein they compared participants' comfort on a water-retaining pavement with a relatively higher reflectance with that on a dense asphalt pavement. This was an attempt to combine the cooling benefits of both reflective and evaporative pavements and evaluate their effects from both objective and subjective perspectives. In that study, to determine the influence of the pavement environment on human-thermal comfort, the authors developed an indicator named 'human-thermal load' based on the human-energy balance, which could be applied to situations involving non-uniform environments such as pavements. Their experimental results suggested that reflected solar radiation from highly reflective pavements can potentially increase the thermal load of humans depending on their conditions. Several studies have pointed out that reflective surfaces have limitations [16,17]. Unlike rooftop installations, reflective pavements reflect solar radiation on pedestrians and other urban surfaces, resulting in decreased human-thermal comfort and even increased urban-thermal loads, for example, due to increased energy use. These studies suggest that pavements should be optimized depending on reflectance, ambient conditions, and required outcomes.

In this study, as a stepping stone to future research to optimize the combined effect of reflectance and evaporation, we investigated the effect of a foamed thermal environment on a novel water-retaining pavement to investigate the effect of reflectance on humans during daytime. We mainly evaluated the ambient radiation over water-retaining pavements as outdoor heat exposure is conceptualized by radiation. The obtained results were compared with those obtained for other pavements.

2. Materials and methods

2.1. Pavements

Three distinct pavements were constructed close to each other at the Okayama Prefectural University campus (34°40'N, 135°45'E) in Japan (Fig. 1). The dimensions of each pavement were 7.0 m × 7.0 m, and the location of the test was an open space. Two pavements were characterized as water-retaining pavements based on their reflectances, and the third was a conventional dense-asphalt pavement. In addition to a previously evaluated water retaining pavement, we developed a pavement using a water-retaining material with a relatively lower reflectance. We tried to ensure that the water retaining characteristics of both the two water-retaining pavements were as similar as possible. Both water-retaining pavements were interlocking block pavements that used water-retentive permeable blocks containing fine voids to hold water. Reflectance was determined using a field evaluation method [18], and



Fig. 1. Experimental site (view from south to north).

the pavements are referred to as WR25 (25% reflectance) and WR13 (13% reflectance), depending on their reflectance values. The dense-asphalt pavement (8% reflectance) is denoted by AS. Reflectance was determined under fully wet conditions for both WR25 and WR13, and for AS it was determined without artificial control. The characteristics of the pavements are listed in Table 1.

2.2. Evaluation

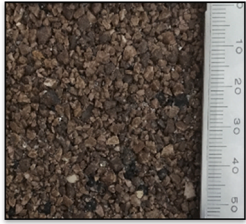
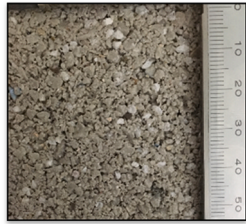

2.2.1. Experimental design

The human-thermal environment on pavements were assessed in three different ways: (a) "Environmental physical quantities," based on measuring climatic and pavement conditions, (b) "Human thermal states," based on physiological quantities and estimating heat stress by the human-thermal load method [15,19], and (c) "Thermal perceptions," based on the participants' responses expressing satisfaction or dissatisfaction with the sensations under the prevailing conditions of the pavements. Field measurements on the three pavements were performed simultaneously during the period from July 24 to August 2, 2017 (summer) during 8:30–15:30 h. A previous study showed that impervious urban surfaces such as asphalt pavements generally dry up in a very short period after rain and thus the evaporation from AS can be negligible [20]. Therefore, water was not sprinkled on the asphalt pavement. Water was sprinkled on the two WR pavements until the WR blocks no longer retained it to ensure uniformity of conditions before each experiment. Since it was difficult to quantify the degree of wetness (or wet condition) of the paved surfaces, we visually reviewed the condition of the surfaces during water sprinkling to ensure that they were fully wet. For reference, the average amount of water sprinkled was 190 L for each WR pavement. Then, human participants were observed for 30 min, after they adapted to the environment for 10 min. All the measurements were performed in a single session. Each subject drank 200 mL of water for 30 min before the experiment to ensure the required level of hydration.

2.2.2. Environmental physical quantities

The surrounding environmental factors were measured at 1 min intervals. These factors included global- and ground-reflected solar radiation, atmospheric- and ground-sourced infrared radiation (MR-60 Net Radiometer, EKO Instruments Co., Ltd., Tokyo, Japan), 3-D wind velocity (CYG-81000 Ultrasonic Anemometer, R.M. Young Co., Traverse City, MI, USA), air temperature and humidity (TR-73U barometric pressure, humidity and temperature recorder, A&D Co., Ltd., Tokyo, Japan), and black globe temperature (Vernon type of 150 mm diameter with T-type thermo-couple, Sibata Scientific Technology Ltd., Saitama,

Table 1
Characteristics of pavements.

	WR13	WR25	AS
Materials	WR block	WR block	Asphalt mixture
Block size (m ²)	0.4 × 0.4	0.2 × 0.1	
Thickness (m)	0.06	0.06	0.04
Appearance	 Brown	 White	 Black
Solar reflectance (%)	13	25	8
Maximum water retention capacity (kg/m ³)	9.14	8.76	

Japan). Air temperature, humidity, and black-globe temperature were measured vertically at 0 (just above the ground surface), 0.35, 0.7, and 1.0 m height, and the rest of the factors were measured at 1.0 m height. This 1.0 m height represents the mid-point of pedestrian height. Considering that our participants were Japanese, the mid-point was considered to be at 1.0 m rather than at 1.1 m height based on ISO 7726. Air temperature and humidity sensors were placed in shelter-tubes with a ventilator to prevent solar radiation effects.

Surface temperatures at five points on the pavements were measured at 1-min intervals using J-type thermocouples. A thermocouple was placed at the center of the pavement, and four thermocouples were placed 0.5 m away from the center of the pavement in the north, east, south, and west directions. Infrared images were periodically captured during the experiment using thermography (InfReC H2640, Nippon Avionics Co., Yokohama, Japan) to ensure temperature uniformity over the surfaces.

The ranges and accuracies of the instruments measuring the environmental physical quantities are summarized in Table 2. Since the uncertainty for measurements of solar radiation and infrared radiation depends on many factors, please refer to the instrument specification for a complete description (<https://eko-usa.com>).

2.2.3. Human thermal states

The human-thermal load is an objective value indicating heat stress based on a formula for calculating the energy balance of the human body. The human-thermal load was calculated from environmental quantities and the physiological reactions of the participants. The human-thermal load (Q) is the heat flux from/to the human body in each condition, and it is defined by Equation (1) as the remaining amount of each item of energy balance [15,19].

Table 2
Measured range and accuracy of the instruments.

	Instrument	Range	Accuracy
Air temperature	TR-73U, thermistor	0–50 °C	±0.3 °C
Humidity	TR-73U, capacitive hygrometer	10–95% R.H.	±5% R.H. @25 °C, 50% R. H.
Solar radiation	MR-60, pyranometer	Second class (ISO9060)	
Infrared radiation	MR-60, pyrgeometer	Second class (ISO9060)	
Wind velocity	CYG-81000, ultrasonic anemometer	0–30 m/s	±0.05 m/s
Black-globe thermometer	Thermocouple, T-type	−40–125 °C	±0.5 °C
Surface temperature	Thermocouple, J-type	−40–375 °C	±1.5 °C

$$Q = M - W + R_{\text{net}} - E - C \quad (1)$$

where the units of all terms are W/m²; M quantifies the metabolic heat generation, W is the workload, R_{net} is the net radiation, E is the evaporative heat loss, and C is the convective heat loss. E is the sum of the wet heat loss from the skin and through respiration; it is determined based on the two-node model [21,22]. C is the sum of the dry heat loss from the skin and through respiration; it is determined based on the ASHRAE model [23]. Each component can be calculated by directly measuring variables such as air temperature, amount of radiation, or skin temperature. For details, refer to previous research [15]. Following the advice of the Research Ethics Committee, metabolic variables for the same posture when standing still were preliminarily determined using an exhaled gas analyzer (VO2000 Electronic Variable Sampling, S & M Co., Ltd., Tokyo, Japan) to prevent excessive load due to wearing masks outdoors.

Rectal and skin temperature at seven points based on the work of Hardy and DuBois [24] (fore-head, upper-arm, hand, abdomen, thigh, lower-leg, and foot) were measured using thermistors (N543 series, Nikkiso-Therm Co., Ltd., Tokyo, Japan, ±0.2 °C accuracy for 0–70 °C range). A heart-rate meter (RS800CX Training Management System, Polar, Kempele, Finland) was installed. All physiological equipment was configured to log data at 1-min intervals. All the participants were dressed in the same outfits: short-sleeve shirts, shorts (Biogear, Mizuno Corporation, Tokyo, Japan), and shoes, which provided a consistent clothing insulation of 0.35 clo or 0.05425 K m²/W [15] throughout the experiment.

Intense outdoor heat gain is caused by radiation. The net radiation of humans is affected by a combination of atmospheric and ground-sourced radiation from by both short-wave (solar) radiation and infrared radiation. Each net-radiation component is expressed as follows:

$$R_{\text{net}_sh} \downarrow = (1 - \alpha_h) R_{sh} \downarrow \quad (2)$$

$$R_{\text{net}_ln} \downarrow = \varepsilon_h \{ R_{ln} \downarrow - \sigma (T_{skin} + 273.15)^4 \} \quad (3)$$

$$R_{\text{net}_sh} \uparrow = (1 - \alpha_h) R_{sh} \uparrow \quad (4)$$

$$R_{\text{net}_ln} \uparrow = \varepsilon_h \{ R_{ln} \uparrow - \sigma (T_{skin} + 273.15)^4 \} \quad (5)$$

where α_h is the reflectance of the human body (= 0.3), ε_h is the emittance of the human body (= 0.97), R_{net_sh} (W/m²) is the net-heat gain from solar radiation, R_{net_ln} (W/m²) is the net-heat gain from infrared radiation, R_{sh} (W/m²) is the heat gain from solar radiation, R_{ln} (W/m²) is the heat gain from infrared radiation, σ (W/m²/K⁴) is the Stefan–Boltzmann constant, T_{skin} (°C) is the mean skin temperature, \downarrow indicates the downward components, and \uparrow indicates the upward components. Finally, the directional net radiation can be obtained as

$$R_{net\downarrow} = R_{net_sh\downarrow} + R_{net_ln\downarrow} \quad (6)$$

$$R_{net\uparrow} = R_{net_sh\uparrow} + R_{net_ln\uparrow} \quad (7)$$

To represent the impact of the direction of irradiation and size of the person on the net radiation, the person was treated as a simplified floating rectangular shape with a body surface area of 1.6 m² facing the sun. Further details are available from a previous study [15].

2.2.4. Subjective perceptions

Since an evaluation of subjective thermal feeling is important in the assessment of human thermal environments, we determined the participants' thermal perceptions using the traditional ASHRAE scale (7-point from "cold (−3)" to "hot (+3)" for thermal sensation, and 5-point from "discomfort (−2)" to "comfort (+2)" for thermal comfort) [23]. Simultaneously, participants' perceptions of the effects of atmospheric and ground-source conditions, upper- and lower-body thermal sensations, and thermal comfort were ascertained. All the perceptions were recorded at 2-min intervals, and a total 16 responses (including a response at 0 min) were obtained for each participant. The subjective responses were recorded using Android tablets using an application developed by us. An example of the questionnaire used in the present study is shown in Figure A in the Appendix.

2.3. Participants

Seventy-eight healthy Japanese male university students volunteered to participate in the study (height 172.6 ± 5.3 cm, weight 64.0 ± 7.5 kg, age 22.4 ± 1.2 yr, and range = mean ± SD). Twenty-six participants engaged in the experiment for each pavement, thus 78 trials were conducted in total. Informed consent was obtained from each participant prior to the experiment. The research was conducted with the approval of the Research Ethics Committee of the Osaka Prefecture University (project title: The relationship between thermal environmental factors and human physiological responses, PI: Atsumasa YOSHIDA, approval date: September 30, 2016).

2.4. Classification of conditions

Solar radiation is the strongest contributor to outdoor thermal environments, and the amount of solar radiation from the sky is influenced by the geography of the observation site, season, time of day, and weather conditions. According to the METPV-20 database of the New Energy and Industrial Technology Development Organization [25], the diffused insolation is less than 300 W/m² at the maximum, and direct insolation is less than 700 W/m². Thus, we have classified cases according to the amount of solar radiation from the sky in addition to the overall conditions as follows: (I) low insolation (overcast), $S < 300$ W/m², (II) medium insolation (partly sunny/cloudy), $300 < S < 700$, and (III) high insolation (clear sky), $S > 700$ W/m². Direct- and diffused-insolation for sunny and cloudy conditions in late July in Okayama are presented in Figure B in the Appendix as a reference.

2.5. Data analysis and comparison

Since the situations were relatively stable during the 30-min period of the experiment, time-mean values were evaluated. Significant differences among distinct pavements were ascertained using the Tukey–Kramer method. The significance level was set to 0.05 ($p < 0.05$).

Several thermal indices are used to assess outdoor-thermal comfort. UTCI is the most comprehensive index for the calculation of heat stress in outdoor spaces [26,27]. Therefore, we analyzed the correlation between human-thermal load and UTCI in terms of thermal sensation for validation.

3. Results and discussion

3.1. General conditions

Results obtained from the experiment are presented in this section.

3.1.1. Climatic quantities

Twenty-six trials were conducted, and the climatic conditions on AS at 1.0-m height are summarized in Table 3 for comparison. The mean values were 33.2 °C for air temperature, 58.4% for relative humidity, 612 W/m² for sky solar radiation, 519 W/m² for sky infrared radiation, and 0.65 m/s for wind speed. These climatic conditions were considered to be typical of the summer conditions in Okayama, as outlined in the database of the Japan Meteorological Agency. However, relatively larger variations were observed in solar radiation, which depends on weather parameters, notably, cloud cover.

3.1.2. Pavement related quantities

Thermal conditions on the experimental pavements are compared in Table 4. The experimental site was an open space, and surface temperatures were uniformly distributed over pavements; thus, mean-surface temperatures during the entire experiment were compared. As reflective pavements tend to absorb less solar energy, surface temperatures were the highest on AS (52.9 °C), lower on WR13 (40.2 °C), and lowest on WR25 (39.4 °C). Thus, the lower was the solar reflectance, the higher was the surface temperature. There were significant differences between the values over AS and those over WR13 and WR25. Both WRs exhibited lower surface temperatures owing to water evaporation, and no significant difference was observed between them.

While ground temperature differed greatly between AS and WRs, air temperature and humidity exhibited similar values for each pavement at 1.0-m height; the air temperature was approximately 33 °C and the relative humidity was 59%. Black-globe temperature is influenced by prevailing environmental factors such as air temperature, wind, and radiant temperature. Moreover, radiant temperature is influenced by downward and upward components of both solar and infrared radiation. Ground-sourced upward radiation components are summarized in Fig. 2. The amount of reflected solar radiation was highest on WR25, was lower on WR13, and the lowest on AS. Infrared radiation from the ground was highest on AS, lower on WR13, and the lowest on WR25, and it was approximately related to surface temperature. Upward radiation was determined by adding both solar and infrared components, and the values were 624 W/m² for WR13, 693 W/m² for WR25, and 694 W/m² for AS. Atmospheric conditions such as solar and infrared radiation and air temperature were almost the same. Black-globe temperatures on AS had marginally higher values probably because they reflect the difference in the ground-sourced radiations; however, the differences among the pavements were not significant.

The effect of height on ambient conditions for each pavement is examined in Fig. 3. Significant differences between AS and both WR13 and WR25 were observed for all physical quantities at a height of 0 m. The resultant air temperature and humidity was dominated by diffusion from the pavement surface and atmospheric conditions. In general, any quantity marginally decreased with increasing distance from the surface, and the effects of the distinct pavements decreased with increasing

Table 3

Summary of climatic quantities (1.0-m height on AS).

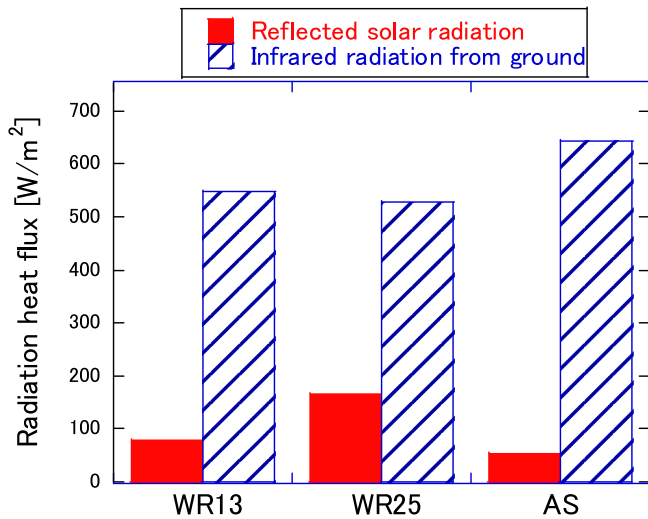
	Mean	Max	Min	S.D.
Air temperature °C	33.2	35.9	29.1	1.6
Humidity %	58.4	72.4	49.3	6.2
Solar radiation from sky W/m ²	612	907	147	229
Infrared radiation from sky W/m ²	519	540	487	14
Wind speed m/s	0.65	1.05	0.40	0.15

S.D., standard deviation.

Table 4

Thermal conditions on each pavement.

	WR13	WR25	AS
Air temperature °C (1.0-m height)	32.8	33.2	33.2
Humidity % (1.0-m height)	59.8	59.4	58.4
Black-globe temperature °C (1.0-m height)	45.7	46.5	47.4
Ground temperature °C	39.4	40.2	52.9

**Fig. 2.** Composition of upward radiation components.

distance from the surface; thus, no significant differences in ambient conditions were observed above the 0.35-m height. In addition, the rise in the humidity over the WRs was not significant; thus, the discomfort induced by evaporation in the vicinity of the pavement surface is expected to be limited.

3.1.3. Human-related quantities and thermal indices

Physiological parameters such as mean-skin and rectal temperatures and subjective perceptions are listed in Table 5. Fig. 4 shows the results of the quantitative evaluation of human-thermal load. Heat stresses exceeded 200 W/m^2 for all pavements. The differences in human-thermal loads among the distinct pavements were caused by differences in net radiation, particularly ground-sourced radiations. Other factors such as metabolic heat (approximately 60 W/m^2) and convective heat (approximately -15 W/m^2), and evaporative heat (approximately -25 W/m^2) showed similar values. Since the environments were under heated conditions, participants dominantly reported experiencing heat

and discomfort ($0 < \text{thermal sensation and thermal comfort} < 0$). However, the values remained almost the same in every quantity, and there was no significant difference among the distinct pavements. The mean skin and rectal temperatures were within the normal range. Owing to variations in atmospheric radiation, the human-thermal load was not significantly different among the three pavements, which is in agreement with physiological and subjective evaluations.

3.2. Foamed environment depending on insolation conditions

Atmospheric insolation conditions for each trial are summarized in Fig. 5. Based on the classification, four trials were conducted under low- (I), 10 in medium- (II), and 12 under high insolation conditions (III). The amounts of sky solar radiation and sky infrared radiation were $230 \pm 56 \text{ W/m}^2$ and 504 ± 11 conditions (I), $505 \pm 109 \text{ W/m}^2$ and 530 ± 16 under condition (II), and $814 \pm 56 \text{ W/m}^2$ and 534 ± 14 under condition (III), respectively. Depending on the weather, sky solar radiation changes widely, however; we observe no significant changes in sky infrared radiation. Amounts of solar radiation were larger than infrared radiation only under condition (III).

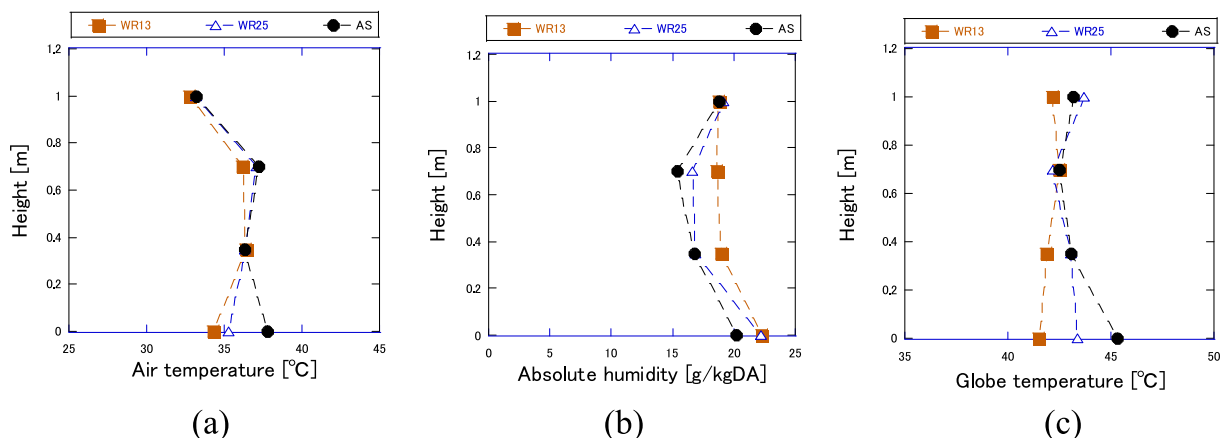
3.2.1. Pavement conditions

Surface temperatures are compared in Fig. 6; temperatures over AS tend to increase with increasing insolation, for instance, 38.5°C under condition (I) and 56.3°C under (III). Surface temperatures over WR13 and WR25 remained at approximately 40°C regardless of insolation. Consequently, the reductions in surface temperatures on WRs compared to those on AS tended to increase with increasing surface temperature on AS. Surface temperatures of the WRs were significantly lower than that of the AS, and a temperature reduction effect of up to 18°C was confirmed for both WRs under condition (III). The reduction in surface-temperature of WRs can be confirmed even under the medium- (approximately 11°C) and low- (approximately 4°C) insolation conditions. Water retention capacity ($\text{WR13} > \text{WR25}$ from Table 1) may affect surface-temperatures under high insolation; the surface temperature on

Table 5

Physiological and perceptual responses.

		WR13	WR25	AS
Physiology	Mean skin temperature °C	36.6	36.6	36.8
	Rectal temperature °C	37.3	37.4	37.4
Perception	Whole-thermal sensation	0.54	0.42	0.66
	Whole-thermal comfort	-0.29	-0.21	-0.35
	Upper-thermal sensation	0.48	0.39	0.59
	Upper-thermal comfort	-0.27	-0.20	-0.33
	Lower-thermal sensation	0.37	0.31	0.50
	Lower-thermal comfort	-0.17	-0.15	-0.26

**Fig. 3.** The effects of height on ambient conditions. (a) Air temperature, (b) Absolute humidity, and (c) Black-globe temperature.

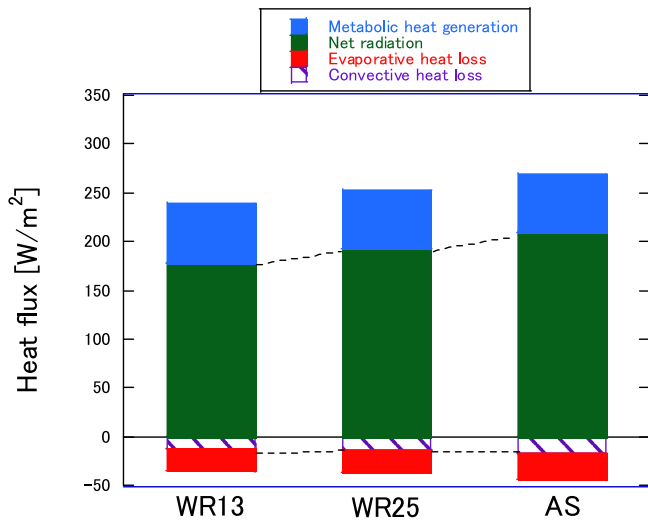


Fig. 4. Human-thermal load components for all conditions.

WR25 was marginally higher than that on WR13; however, there was no significant difference between WR13 and WR25. This is because the humidity in the vicinity of the pavement surface was sufficiently high after water-supply during evaporation and thus there was limited effect from additional evaporation due to higher water retention.

3.2.2. Thermal conditions on pavements

Ambient conditions (air temperature and humidity at 1.0-m height) are summarized in Fig. 7. Because weather conditions depend on sky solar radiation and local weather conditions, they directly affect air temperature. Air temperature at the 1.0-m condition (I) shows lower values, and it is marginally higher in conditions (II) and (III). However, there was no difference among the pavements for each condition. Similarly, we observed no effect of evaporation from the pavement on humidity.

Solar and infrared radiation that are reflected based on the insolation conditions of pavement sources are summarized in Fig. 8. Because the extent of reflected solar radiation is a multiplication of sky solar radiation and reflectance of the surface, WR25 exhibits the highest value among pavements under the same insolation condition owing to its higher reflectance. Because infrared radiation from the ground is influenced by surface temperature, under medium- and high-insolation conditions, AS exhibits significantly larger values compared to both WRs. Additionally, the radiation environment on pavements is evaluated using black-globe temperature in Fig. 8 (c). Although pavements affect radiation environments by determining both upward solar and

infrared radiation components, solar radiation from the sky is a stronger heat source and it is dominant under the sun. Therefore, black-globe temperature is higher with higher insolation (approximately 48 °C) and lower with lower insolation (approximately 38 °C) but shows similar values on distinct pavements within each insolation condition.

3.2.3. Human-thermal conditions

A comparison of whole-body human-thermal load is compared in Fig. 9. Clear differences exist in the human-thermal load depending on insolation. The values between AS and WR under conditions (I) and (II) were not significant. Human-thermal load on WR13 was 215 W/m², and the difference in the human-thermal load became obvious as insolation increased. The differences were 61 and 18 W/m² between WR25 and AS and AS and WR13 under condition (III), respectively. The cause for each human-thermal load component was shown in Fig. 9 (b) and (c). A comparison between low- and high-insolation indicates a decisive difference in the net radiation component. Sky solar radiation makes a fundamental difference in human-thermal load, and the net radiation on each pavement under condition (I) is 80–100 W/m². On the other hand, the net radiation under condition (III) was 197, 243, and 265 W/m² for WR13, WR25, and AS, respectively. Other factors such as metabolic heat (approximately 60 W/m²) and convective heat (approximately -15 W/m²), and evaporative heat (approximately -25 W/m²) show similar values. Conditions were almost the same and they did not directly affect sensible and latent heat losses. For a detailed analysis, we classified net

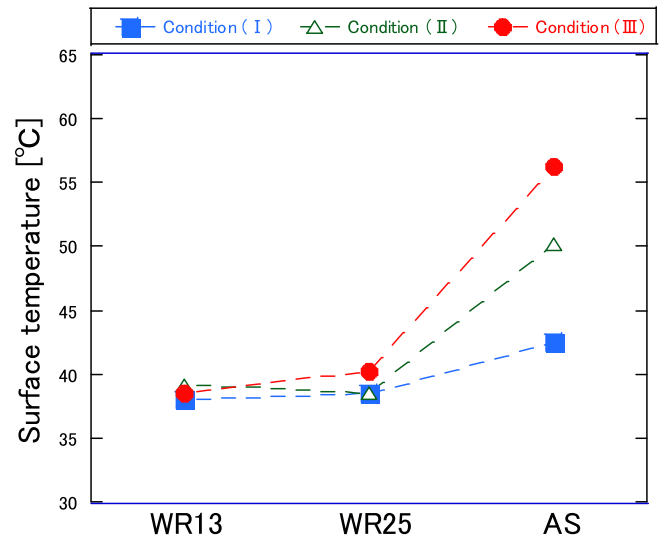


Fig. 6. Surface temperatures based on insolation conditions.

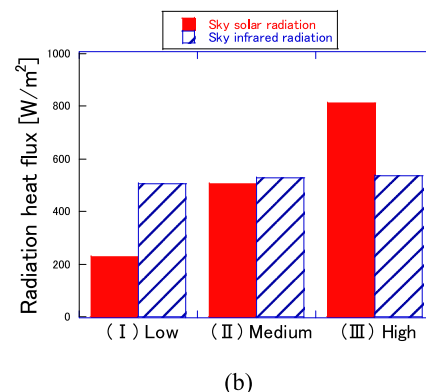
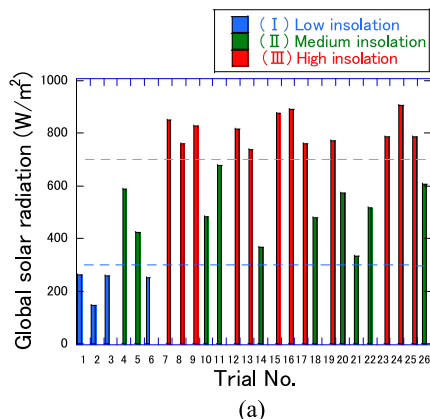


Fig. 5. Radiative conditions. (a) Classification and (b) Composition of atmospheric radiation components.

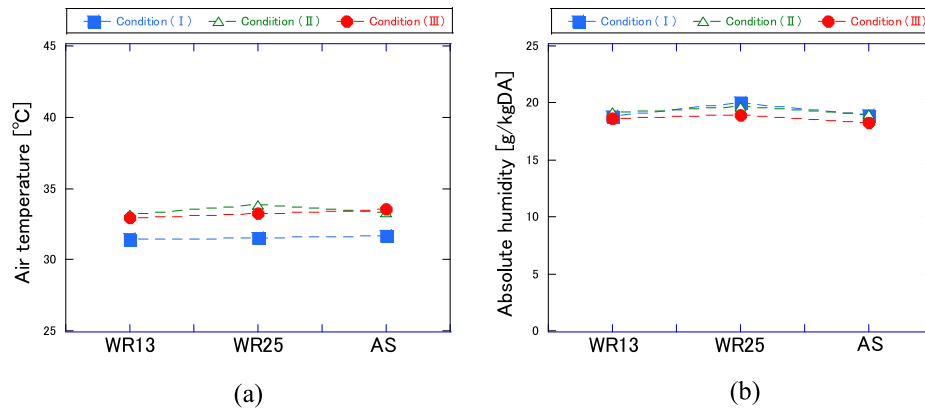


Fig. 7. Ambient (insolation) conditions. (a) Air temperature and (b) Absolute humidity.

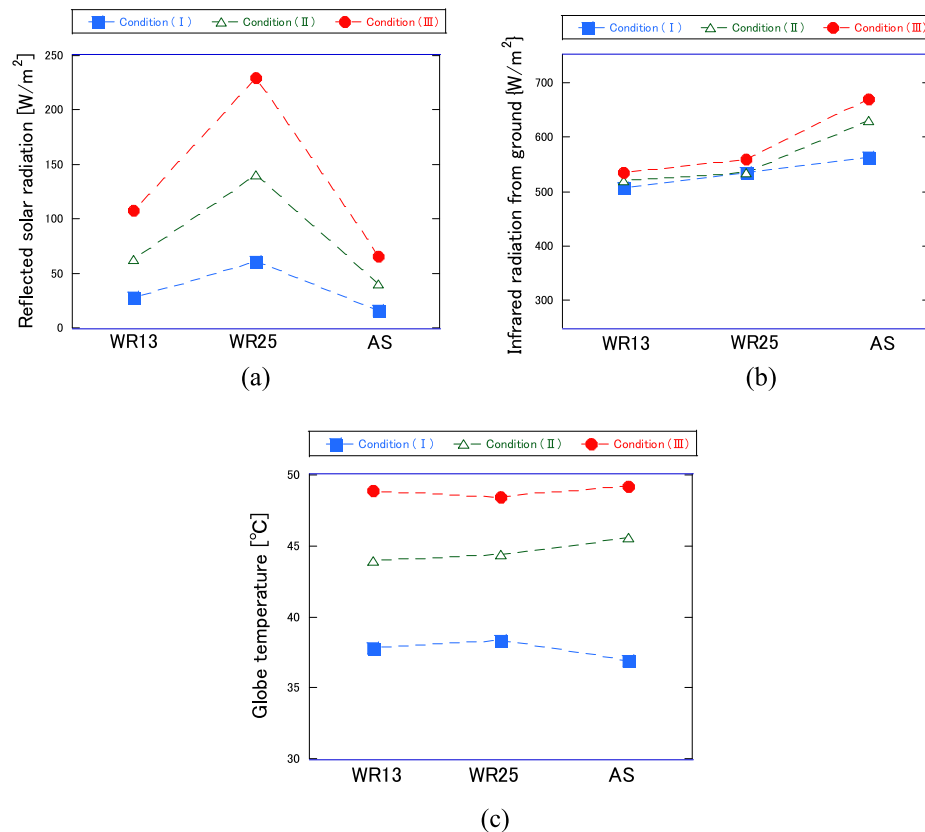


Fig. 8. Radiative environment based on insolation conditions. (a) Reflected solar radiation, (b) Infrared radiation, and (c) Globe temperature.

radiation into sky-sourced downward and pavement-sourced upward components, as shown in Fig. 9 (d) and (e). Although the amount of each radiation component varies among the conditions, atmospheric downward solar radiation is the most influential component in any condition. Under low insolation, total radiation heat gain is relatively small, and the difference among the pavements has a limited effect. However, the balance between ground-sourced upward solar and infrared radiation differs under high insolation. In AS, there is a smaller reflected solar radiation but a larger ground infrared radiation. The balance is opposite on WR25; there is a larger reflected solar radiation but a smaller ground infrared radiation. WR13 receives moderate heat from both ground reflected and infrared radiation, and thus, it exhibits the lowest total net radiation, and consequently, the lowest human-thermal load.

Subjective perceptions are summarized in Fig. 10. Since the environments were under heated conditions, participants expressed hotter

and more uncomfortable conditions, and thermal comfort was inversely correlated with that of thermal sensation. As a result, a significant difference among distinct pavements can be seen only under condition (III) for lower-body thermal sensation and comfort and whole-body thermal sensation and comfort. As the environment differs between different parts of the human body (particularly, the lower hemisphere) located in closer proximity to ground level, the environmental difference that is induced by foamed pavements resulted in significant differences in thermal sensation and thermal comfort between WR13 and AS for the lower body. These differences may cause significant differences even at the whole-body level. Thermal sensation in improvement was reported even on WR25, compared to AS at the whole-body level. Thermal sensation and thermal comfort are cooler and more comfortable for the lower-body, and this is explained by the composition of human-thermal load or the radiation balance between the upward and downward

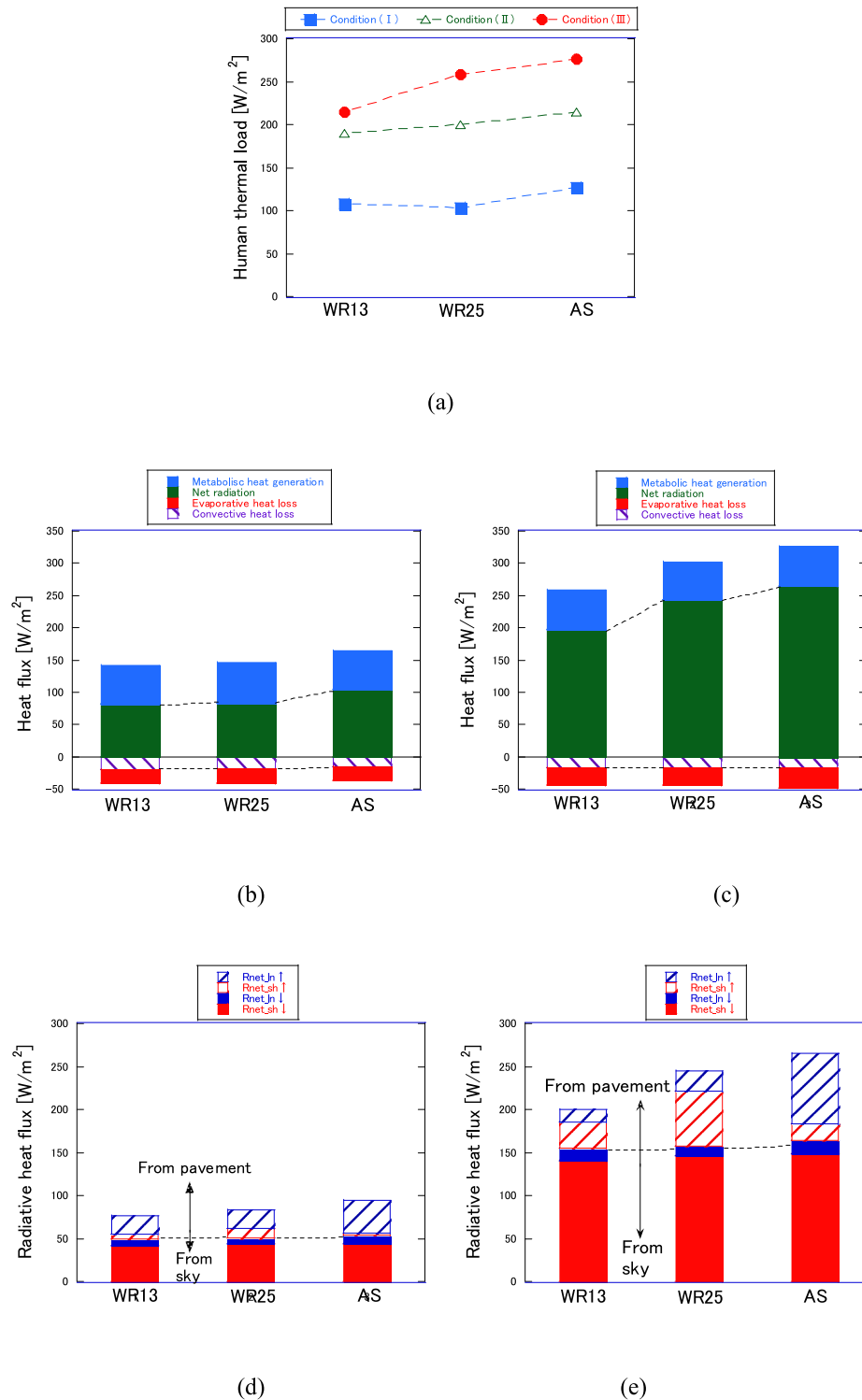


Fig. 9. Detailed analysis based on human-thermal load index. (a) Total human-thermal load, (b) Human-thermal load components in condition (I), (c) Human-thermal load components in condition (III), (d) Composition of net radiation in condition (I), and (e) Composition of net radiation in condition (III).

component in Fig. 9. The ground-sourced upward component is smaller than the downward component at high insolation. Interestingly, thermal sensation and thermal comfort seem to follow the degree of thermal load on different parts of the body; consequently, thermal sensation is the smallest for the lower body and the highest for the whole-body.

Physiological parameters may support these results. Skin temperature distributions under condition (III) are shown in Fig. 10 (b), and the mean skin and rectal temperatures are listed in Table 6. Skin

temperatures in the lower anatomical regions such as the thigh, lower leg, and foot were influenced by an improvement in the thermal environment in the vicinity of WR13, and they are significantly lower on WR13 compared to AS. Mean skin temperature on WR13 was significantly lower than that on AS; however, no effect was observed on rectal temperature owing to the under development of heat strain on any pavement.

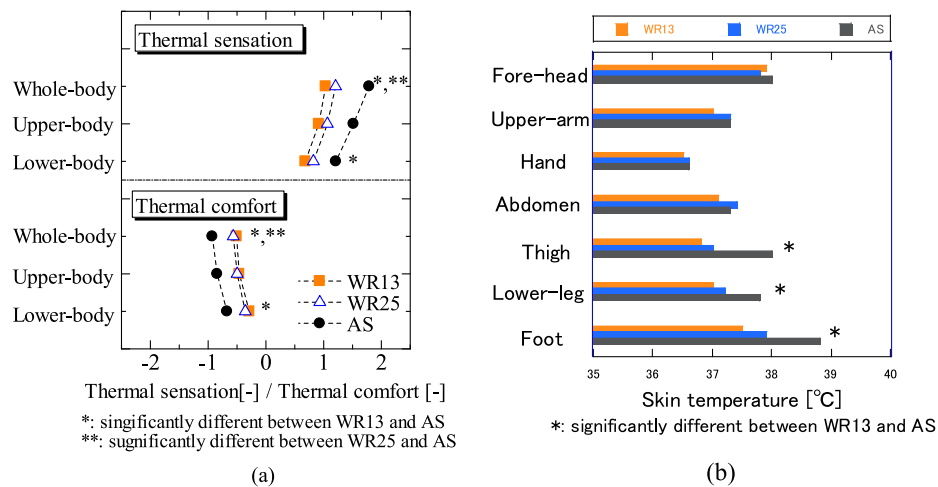


Fig. 10. Human-related measurements. (a) Thermal perception and (b) Skin temperature distributions.

Table 6

Mean-skin and rectal temperatures under high insolation.

	WR13	WR25	AS
Mean skin temperature °C	36.9 *	37.3	37.8 *
Rectal temperature °C	37.4	37.3	37.4

* Significantly different between AS and WR13.

3.3. Validation and application

Water-retaining pavements are proposed as a solution to the UHI problem because they may help to cool cities. Surface temperature is the most common focus of research aiming to evaluate the cooling of cities. Surface-temperatures of WRs were compared with a conventional AS pavement and temperature reductions were confirmed for the overall surfaces of WR, especially at 18 °C under high insolation, and at an above-average level compared to reports of previous studies [28]. Because the hotter surfaces warm the near-surface air, reduction of surface-temperatures of WRs can induce reductions in air temperatures. However, the effects of the WR pavement on air temperature and humidity at a pedestrian height cannot be found in the experiment. According to the literature, while cool pavements can dramatically reduce surface temperatures by up to 20 °C, air temperature is less sensitive, and the reduction is reportedly within 1 °C [29]. As the experiment was conducted for a somewhat longer period but still within a single day, it is possible that daily weather fluctuations may eliminate the differences in air temperature. Because the limited size of the test pavement may have limited the influence of the cooler surfaces on ambient air [30], determining the effective area is an important issue for practical applications. Although the temperature performance of water retaining pavement is a complicated process, understanding it is fundamentally important because of its close relationship to the state of the infrared radiation on the WRs. The effects of specific attribute of materials including water retention, evaporation efficiency, reflectance, and the heat transfer coefficient still remain to be investigated and this is planned for a future study.

Because microclimatic conditions affect the use of outdoor spaces, considering the relationships among the environment, the body's thermal states, and the individual's perceptions, such as thermal sensation and comfort are important considerations for urban design. Simple indices such as WBGT are not suitable for complex radiation environments, such as pavements. In fact, none of the factors affecting WBGT, such as globe and air temperatures, and humidity showed significant differences; however, different subjective responses on distinct pavements were observed. Our analyses used both qualitative and

quantitative methodological approaches. To ensure that our methodology supports human thermal evaluation, the relationship between human-thermal load and thermal sensation is plotted in Fig. 11 (a). Furthermore, we validate that UTCI is calculated and compared with that of thermal sensation. First, plots on WR13 were observed and distributed in the regions with smaller human-thermal load or lower UTCI and relatively cooler sensation, while plots on AS tended to be distributed in regions with larger human-thermal loads or higher UTCI and hotter sensations. The human-thermal load is correlated with thermal sensation, and an almost linear relationship was observed ($r = 0.62$). The comparison between UTCI and thermal sensation showed a correlation, but with a marginally lower correlation coefficient ($r = 0.53$). Human thermal load can offer advantages, including variations in skin temperature in response to the environment. For instance, the effectiveness of cooling from the pavement was observed from the local skin-temperature drop on WR13, resulting in a local thermal sensation and improvement in comfort on WR13. Whereas plots distribute almost within $38 < \text{UTCI} < 46$. A strong heat stress range corresponding to the thermal stress level for UTCI, thermal sensation responses from below 1 (slightly warm) to 2 (warm). Perceptions may be affected by the participants' adaptation to Japanese hot- and humid-summer weather. Because human-thermal load and UTCI can determine the difference in the human-thermal environment on pavements along with perceptual responses, the method utilizing analysis focusing on the radiative environment and human-thermal load can be used for the evaluation of the outdoor-thermal environment. However, the applicability of the quantitative models related to human-thermal load needs to be carefully considered. Although we considered a person to approximate a simple cuboid structure for the radiation calculation, more accurate methods of predicting the radiation received by individuals in outdoor environments would be beneficial. We used a physiological prediction model based on the two-node model for indoor thermal environments. A recent study successfully revealed the dynamics of thermoregulation in outdoor environments [31]; therefore, our future work will focus on adopting this method to calculate human-thermal load. Accurate assessment of the thermal states of humans involves asking participants directly. Because we were able to determine a good relationship between human-thermal load and thermal sensation, we believe that this validates our results. Furthermore, this study was limited to the evaluation of summer-heat mitigation using Japanese participants; therefore, regression lines may change for universal environments and different participants.

Pedestrian heat exposure is strongly influenced by radiation during the daytime; unfortunately, the radiation environment on pavement for humans has attracted less attention. In Fig. 9, human heat gain increases

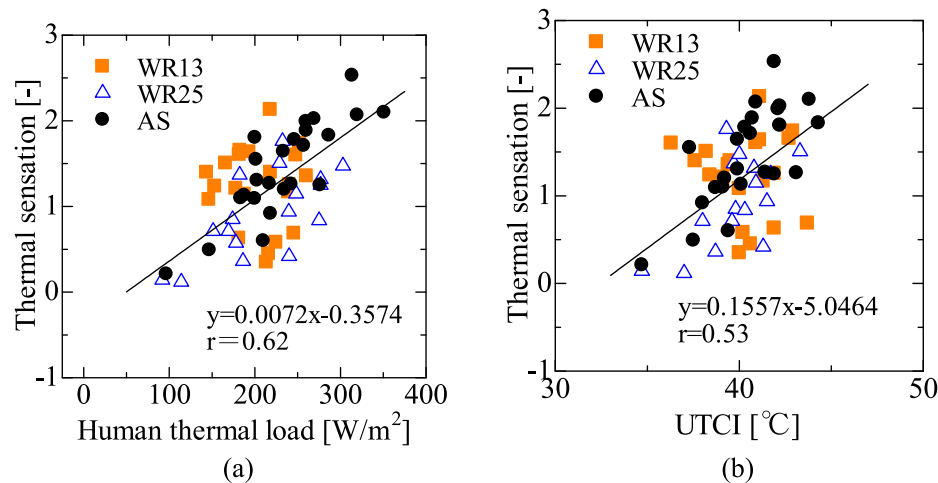


Fig. 11. Relationship of thermal sensation to (a) Human-thermal load and (b) UTCI.

depending on the extent of insolation, and about 50–75% of the heat gain is from the radiation flux (net radiation). Net radiation is the only component that changes dramatically depending on the situation. Highly reflective materials in general reduce surface temperature, for example, ground-sourced infrared radiation; however, they increase reflected solar radiation, and the differential between these radiations is important. Our experiments show that the effects of distinct reflectance materials on foamed thermal and radiative environments did not differ significantly below a certain level of sky solar radiation (700 W/m^2). Under less than moderate insolation, or other than in summer, the reflection characteristics of the WR pavement have little effect, with a lower reflectance than is effective under high insolation. Modest reflective pavements such as WR13 should be preferred for all conditions. Darker-colored water-retaining pavements can be called human-friendly pavements under severe heat and are now installed and utilized for spaces where people gather, such as park and station squares and pedestrian sidewalks; for example, in the surroundings of Japan's new National Stadium where the 2020 Tokyo Olympics and Paralympic Games were held [32]. Lighter-colored reflective pavements have other disadvantages in terms of esthetics and visibility from unacceptable glare [33]. The benefit of water-retaining pavements, regardless of their reflection characteristics, is to keep the surfaces, and consequently humans, cooler even under strong heat exposure, unlike normal, dry, reflective pavement. People can choose color tone to a certain extent, for example to blend in with the surrounding scenery. Differences among installation sites, such as climate, solar angle, and urban morphology are the result of site-dependent features, and therefore, WR pavements are only a partial solution that should be considered in combination with other changes to improve the human living environment. An understanding of the environmental performance of combinations of pavement materials and other urban factors, and their impacts on reducing the UHI remains to be investigated in future. These findings provide a basis for optimizing future experimental designs when investigating applications on larger scales.

These results were obtained using WR pavements that were saturated. Since the performance of WR pavements may differ depending on the wetness, the possible interactions between reflectance and evaporative cooling should be examined. The duration of evaporative cooling is reported to last from a few days [30] to one week [11]. Japan has abundant rainfall, and to simulate that, adequate water was supplied before each experiment. Researchers and a municipal government in Japan experimented with another watering method to effectively maintain the cooling effects from pavements [34]. In our future work we propose to investigate the durability of the cooling effect and watering method, in order to optimize water supply.

4. Conclusions

Cities can reduce thermal load by modifying pavement materials for color and water permeability. WR pavements help improve ambient and human thermal conditions and human comfort under heated conditions. We quantitatively estimated the health benefits of implementing UHI mitigation measures in the surrounding environment using WR pavements with different reflectance values. The subjective field-based measurements lead to the following conclusions:

- (1) Because variations in weather and radiation are major contributors to outdoor environments, classification based on the extent of insolation is beneficial for thermal evaluation under heated conditions.
- (2) Both WR pavements exhibited reduced surface-temperatures compared to the temperatures over AS, regardless of reflectance, under any insolation condition. However, the air temperature and humidity over the pavements were less sensitive to the pavement type, and therefore, they were not significantly affected by distinct pavements.
- (3) We found a good agreement between human-thermal load and thermal sensation, suggesting this as a suitable method for analyzing human-thermal load in order to evaluate the outdoor human-thermal environment. Human-thermal loads on WR pavements differed significantly from those on AS under high-insolation conditions: 215 W/m^2 for WR13, 258 W/m^2 for WR25, and 276 W/m^2 for AS.
- (4) On WR13 under high-insolation conditions, local thermal sensation, comfort and local skin temperature of the lower body improved, which subsequently improved whole-body perception and temperature, likely due to human responses to the thermal environment on WR13 pavement.
- (5) Net radiation accounts for approximately 50–75% of heat gain in the human-thermal load. With regards to the balance of radiation components, both ground-reflected and infrared radiation are received by humans over WR13 in moderate amount. This indicates that the highest reduction performance in human-thermal load can be compared to that of AS. The increasing effect of reflective materials on the foamed thermal and radiation environments is not significant below a certain level of insolation; therefore, a modest reflective pavement, such as WR13, is anticipated to improve the human-thermal environment. Thus, infrared radiation is represented by the reduction in the expected lower surface.

Funding source

This work was partly supported by JSPS KAKENHI Grant-in-Aid for Young Scientists [grant number 17K18026, P.I. Yasuhiro Shimazaki] and Grant-in-Aid for Scientific Research (A) [grant number 17H00802, P.I. Atsumasa Yoshida].

CRediT authorship contribution statement

Yasuhiro Shimazaki: Conceptualization, Data curation, Formal analysis, Funding acquisition, Investigation, Methodology, Validation, Visualization, Writing – original draft, Writing – review & editing. **Masashige Aoki:** Resources, Data curation, Conceptualization. **Kenji**

Karaki: Data curation, Methodology. **Atsumasa Yoshida:** Validation, Supervision, Project administration, Funding acquisition.

Declaration of competing interest

The authors declare that they have no known competing financial interests or personal relationships that could have appeared to influence the work reported in this paper.

Acknowledgment

The authors would like to thank Jumpei Nitta of Okayama Prefectural University for technical assistance with the experiments.

Appendix

2017011_test.txt : 0 min (Response time)

00:12 (Elapsed time) (Sliding bar)

寒い (Cold) 暑い (Hot)

全身温冷感 (Whole-body thermal sensation)

不快 (Discomfort) 快適 (Comfort)

全身快感 (Whole-body thermal comfort)

寒い (Cold) 暑い (Hot)

上半身温冷感 (Upper-body thermal sensation)

不快 (Discomfort) 快適 (Comfort)

上半身快感 (Upper-body thermal comfort)

寒い (Cold) 暑い (Hot)

下半身温冷感 (Lower-body thermal sensation)

不快 (Discomfort) 快適 (Comfort)

下半身快感 (Lower-body thermal comfort)

ANSWER

Fig. A. Example of the questionnaire for 0 min (Original Japanese language is translated into English in the parentheses for a reference).

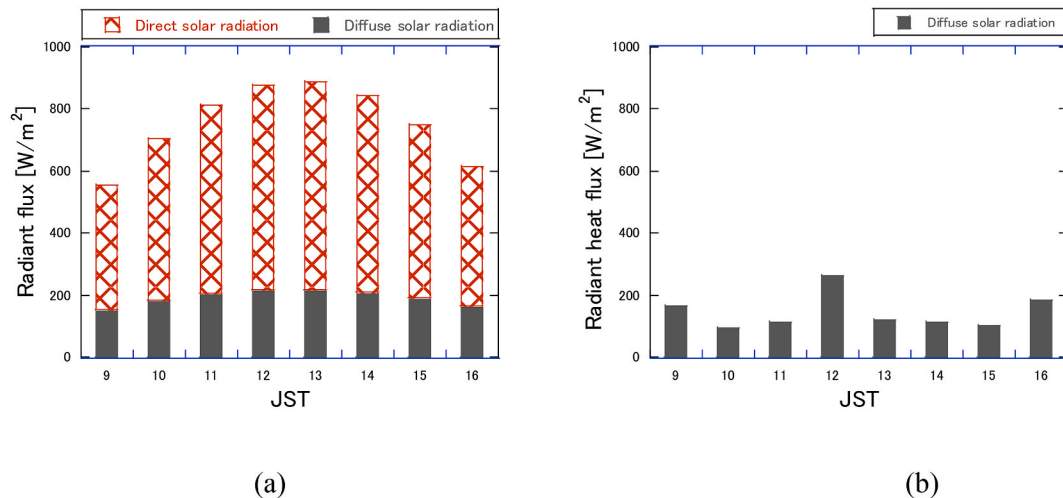


Fig. B. Insolation database at experimental site. (a) Clear sky and (b) Overcast.

References

- [1] S.E. Perkins-Kirkpatrick, S.C. Lewis, Increasing trends in regional heatwaves, *Nat. Commun.* 11 (2020) 3357, <https://doi.org/10.1038/s41467-020-16970-7>.
- [2] S. Hajat, T. Kosatky, Heat-related mortality: a review and exploration of heterogeneity, *J. Epidemiol. Community Health* 64 (2010) 753–760, <https://doi.org/10.1136/jech.2009.087999>.
- [3] B.J. He, Towards the next generation of green building for urban heat island mitigation: zero UHI impact building, *Sustain. Cities Soc.* 50 (2019), <https://doi.org/10.1016/j.scs.2019.101647>, 101647.
- [4] T.R. Oke, *Boundary Layer Climates*, second ed., Routledge, London, U.K., 2002.
- [5] S.Q.S. Hirashima, A. Katschnner, D.G. Ferreira, E. Sd Assis, L. Katschnner, Thermal comfort comparison and evaluation in different climates, *Urban Clim.* 23 (2018) 219–230, <https://doi.org/10.1016/j.uclim.2016.08.007>.
- [6] H. Akbari, M. Pomerantz, H. Taha, Cool surfaces and shade trees to reduce energy use and improve air quality in urban areas, *Sol. Energy* 70 (3) (2001) 295–310, [https://doi.org/10.1016/S0038-092X\(00\)00089-X](https://doi.org/10.1016/S0038-092X(00)00089-X).
- [7] A. Synnefa, A. Dandou, M. Santamouris, M. Tombrou, N. Soulaekellis, On the use of cool materials as a heat island mitigation strategy, *J. Appl. Meteorol. Climatol.* 47 (11) (2008) 2846–2856, <https://doi.org/10.1175/2008JAMC1830.1>.
- [8] S. Bretz, H. Akbari, A. Rosenfeld, Practical issues for using solar-reflective materials to mitigate urban heat islands, *Atmos. Environ.* 32 (1) (1998) 95–101, [https://doi.org/10.1016/S1352-2310\(97\)00182-9](https://doi.org/10.1016/S1352-2310(97)00182-9).
- [9] H. Li, *Pavement Materials for Heat Island Mitigation: Design and Management Strategies*, Butterworth-Heinemann, Waltham MA, 2016.
- [10] M. Santamouris, Using cool pavements as a mitigation strategy to fight urban heat island—a review of the actual developments, *Renew. Sustain. Energy Rev.* 26 (2013) 224–240, <https://doi.org/10.1016/j.rser.2013.05.047>.
- [11] Y. Qin, A review on the development of cool pavements to mitigate urban heat island effect, *Renew. Sustain. Energy Rev.* 52 (2015) 445–459, <https://doi.org/10.1016/j.rser.2015.07.177>.
- [12] M. Hendel, P. Gutierrez, M. Colombero, Y. Diab, L. Royon, Measuring the effects of urban heat island mitigation techniques in the field: application to the case of pavement-watering in Paris, *Urban Clim.* 16 (2016) 43–58, <https://doi.org/10.1016/j.uclim.2016.02.003>.
- [13] N. Yaghoobian, J. Kleissl, Effect of reflective pavements on building energy use, *Urban Clim.* 2 (2012) 25–42, <https://doi.org/10.1016/j.uclim.2012.09.002>.
- [14] D. Lai, D. Guo, Y. Hou, C. Lin, Q. Chen, Studies of outdoor thermal comfort in northern China, *Build. Environ.* 77 (2014) 110–118, <https://doi.org/10.1016/j.buildenv.2014.03.026>.
- [15] Y. Shimazaki, M. Aoki, J. Nitta, H. Okajima, A. Yoshida, Experimental determination of pedestrian thermal comfort on water-retaining pavement for UHI adaptation strategy, *Atmosphere* 12 (2021) 127, <https://doi.org/10.3390/atmos12020127>.
- [16] S. Sen, L. Khazanovich, Limited application of reflective surfaces can mitigate urban heat pollution, *Nat. Commun.* 12 (2021) 3491, <https://doi.org/10.1038/s41467-021-23634-7>.
- [17] A. Middel, V.K. Turner, F.A. Schneider, Y. Zhang, M. Stiller, Solar reflective pavements—A policy panacea to heat mitigation? *Environ. Res. Lett.* 15 (6) (2020) <https://doi.org/10.1088/1748-9326/ab87d4>.
- [18] Y. Shimazaki, A. Yoshida, Y. Satsumoto, S. Taketani, Effect of properties of sports surface and clothing materials on human-thermal load under hot environment, *Procedia Eng.* 72 (2014) 502–507, <https://doi.org/10.1016/j.proeng.2014.06.087>.
- [19] Y. Shimazaki, A. Yoshida, R. Suzuki, T. Kawabata, D. Imai, S. Kinoshita, Application of human-thermal load into unsteady condition for improvement of outdoor thermal comfort, *Build. Environ.* 46 (8) (2011) 1716–1724, <https://doi.org/10.1016/j.buildenv.2011.02.013>.
- [20] H. Takebayashi, M. Moriyama, Study on surface heat budget of various pavements for urban heat island mitigation, *Adv. Mater. Sci. Eng.* (2012) 523051, <https://doi.org/10.1155/2012/523051>, 2012.
- [21] A.P. Gagge, J.A.J. Stolwijk, Y. Nishi, An effective temperature scale based on a simple model of human physiological regulatory response, *ASHRAE Trans.* 77 (1971) 247–262.
- [22] A.P. Gagge, A.P. Fobelets, L.G. Berglund, A standard predictive index of human response to the thermal environment, *ASHRAE Trans.* 92 (1986) 709–731.
- [23] ASHRAE, *ASHRAE Handbook: Fundamentals*, ASHRAE, Atlanta, 2017.
- [24] J.D. Hardy, E.F. Du Bois, G.F. Soderstrom, The technic of measuring radiation and convection, *J. Nutr.* 15 (5) (1938) 461–475, <https://doi.org/10.1093/jn/15.5.461>.
- [25] (in Japanese), <https://www.nedo.go.jp/index.html>.
- [26] G. Jendritzky, R. de Dear, G. Havenith, UTCI, UTCI—Why another thermal index? *Int. J. Biometeorol.* 56 (2012) 421–428, <https://doi.org/10.1007/s00484-011-0513-7>.
- [27] S. Zare, N. Hasheminejad, H.E. Shirvan, R. Hemmatjo, K. Sarebazzadeh, S. Ahmadi, Comparing Universal Thermal Climate Index (UTCI) with selected thermal indices/environmental parameters during 12 months of the year, *Weather Clim. Extremes* 19 (2018) 49–57, <https://doi.org/10.1016/j.wace.2018.01.004>.
- [28] M. Hendel, Pavement-watering for cooling the built environment: a review, HAL (open archive), hal-01426167, <https://hal.archives-ouvertes.fr/hal-01426167/document>, 2016.
- [29] T. Nakayama, T. Fujita, Cooling effect of water-holding pavements made of new materials on water and heat budgets in urban areas, *Landsc. Urban Plann.* 96 (2010) 57–67, <https://doi.org/10.1016/j.landurbplan.2010.02.003>.
- [30] J. Wang, Q. Meng, K. Tan, L. Zhang, Y. Zhang, Experimental investigation on the influence of evaporative cooling of permeable pavements on outdoor thermal environment, *Build. Environ.* 140 (2018) 184–193, <https://doi.org/10.1016/j.buildenv.2018.05.033>.
- [31] V. Melnikov, V.V. Krzhizhanovskaya, M.H. Lees, P.M.A. Sloom, System dynamics of human body thermal regulation in outdoor environments, *Build. Environ.* 143 (2018) 760–769, <https://doi.org/10.1016/j.buildenv.2018.07.024>.
- [32] NIHON KOGYO Co., Ltd., NIKKOWORKS, http://www.nihon-kogyo.co.jp/dream/kanto/images/20200501_kokuritsu.pdf, 2020.
- [33] N. Xie, H. Li, A. Abdelhady, J. Harvey, Laboratorial investigation on optical and thermal properties of cool pavement nano-coatings for urban heat island mitigation, *Build. Environ.* 147 (2019) 231–240, <https://doi.org/10.1016/j.buildenv.2018.10.017>.
- [34] H. Takebayashi, H. Danno, U. Tozawa, Study on appropriate heat mitigation technologies for urban block redevelopment based on demonstration experiments in Kobe city, *Energy Build.* 250 (2021) 111299, <https://doi.org/10.1016/j.enbuild.2021.111299>.